

Structure and magnetoelectric coupling of $\text{LiNi}_{1-x}\text{Co}_x\text{PO}_4$ multiferroics

M.A. Semkin¹, N.V. Urusova^{1,2}, M.O. Kalinkin², N.A. Kulesh¹, D.K. Kuznetsov¹,
D.S. Neznakhin¹, A.S. Volegov^{1,3}, D.G. Kellerman^{1,2}, A.N. Pirogov^{1,3}

¹*School of Natural Sciences and Mathematics, Ural Federal University, 620000, Ekaterinburg, Russia*
m.a.semkin@urfu.ru

²*Institute of Solid State Chemistry of the Ural Branch of the RAS, 620990, Ekaterinburg, Russia*

³*M.N. Mikheev Institute of Metal Physics of the Ural Branch of the RAS, 620108, Ekaterinburg, Russia*

Lithium orthophosphates LiMPO_4 , where $M = (\text{Ni}, \text{Co}, \text{Mn}, \text{Fe})$ crystallize to olivine structure, the space group is $Pnma$. They exhibit multiferroic properties with high linear magnetoelectric effect $\alpha \leq 2.0$ pS/m [1, 2]. Excepting LiNiPO_4 , in other LiMPO_4 there is with temperature only a transition from a commensurate antiferromagnetic phase to a paramagnetic state. The polarization arises at the temperature that is equal to the Neel point (T_N) [3]. This fact indicates a strong interaction between magnetic and ferroelectric degrees of freedom. In LiNiPO_4 a polarization exists only in the temperature interval, where the commensurate magnetic phase takes place [4]. Further heating of the sample induces magnetic phase transition to an incommensurate structure at $T_{C-IC} = 20.8$ K and then to the paramagnetic state at $T_N = 21.8$ K. The commensurate antiferromagnetic structure of the orthophosphates LiMPO_4 with $M = (\text{Ni}, \text{Co}, \text{Mn}, \text{Fe})$ is described by the propagation vector $\mathbf{k} = 0$. For example, in the case of the commensurate structure of LiNiPO_4 magnetic moments of Ni ions, located at positions $(0.25 + x, 0.25, -z)$ and $(0.25 - x, -0.25, 0.5 - z)$, are oriented along the c -axis and antiparallel to each other as well as to the moments at sites $(-0.25 - x, -0.25, z)$, and $(-0.25 + x, -0.25, 0.5 + z)$; where $x = 0.026$, $z = 0.018$ [5]. The commensurate structures of other orthophosphates differ from this structure for a mutual orientation of moments or their directions relatively the crystallography axes. For instance, the spins are oriented along the a -axis for LiMnPO_4 , and along the b -axis for LiCoPO_4 [6, 7].

In our work we present the results of structure and magnetic measurements of $\text{LiNi}_{1-x}\text{Co}_x\text{PO}_4$ multiferroic where $x = (0, 0.1, \dots, 0.7)$, and there analysis depend on concentration (x). The $\text{LiNi}_{1-x}\text{Co}_x\text{PO}_4$ multiferroics have been synthesized by a glycerol-nitrate method. X-ray diffraction (XRD) measurements were carried out at room temperature using Shumadzu diffractometer (X-ray source $\text{Cu K}\alpha$ $\lambda = 1.5418$ Å). Structural parameters were refined by Rietveld method using Fullprof program. Morphology of the prepared powder samples was identified by scanning electron microscopy (SEM) AURIGA CrossBeam. The chemical composition ($\text{Ni}_{1-x}\text{Co}_x$) was studied using a full reflection Nanohunter X-ray fluorescence spectrometer. Magnetic measurements were performed with Magnetic Property Measurement System (MPMS XL-7) in the temperature range (2–300) K, under the applied magnetic field of 500 Oe, in the zero field cold (ZFC) mode. The (2–25) K and (25–300) K intervals were investigated with the step ~ 0.1 K and 1 K, respectively.

Figure 1 shows the XRD-patterns for $\text{LiNi}_{1-x}\text{Co}_x\text{PO}_4$ with $x = (0, 0.1, 0.2, 0.3, 0.5, \text{ and } 0.7)$, and SEM-image of the $\text{LiNi}_{0.6}\text{Co}_{0.4}\text{PO}_4$ (for example). All observed reflections correspond to the $Pnma$ space group. The structural parameters have been refined; the lattice constants, and global agreement factor presented in Table 1. The size of the unit cell increases with increasing cobalt concentration in $\text{LiNi}_{1-x}\text{Co}_x\text{PO}_4$. The SEM-image shows that $\text{LiNi}_{0.6}\text{Co}_{0.4}\text{PO}_4$ are homogeneous particles with average size from 0.5 up to 5 μm . Similar SEM-images have been recorded for other samples.

For all samples $\text{LiNi}_{1-x}\text{Co}_x\text{PO}_4$ with $x = (0, 0.1, \dots, 0.7)$ the magnetic phase transitions from the commensurate antiferromagnetic phase to the incommensurate antiferromagnetic state, and to the paramagnetic state are observed. The temperature of the magnetic phase transition from the commensurate to the incommensurate structures (T_{C-IC}) were determined from the temperature dependence of the first derivative of the magnetisation for $\text{LiNi}_{1-x}\text{Co}_x\text{PO}_4$ multiferroics, expected that the magnetoelectric coupling will exist below T_{C-IC} temperature, these values presented in Table 1. The T_{C-IC} temperature decreases in the $\text{LiNi}_{1-x}\text{Co}_x\text{PO}_4$ with increasing the cobalt concentration (x) from 0 up to 0.5, and vice versa increase at concentrations

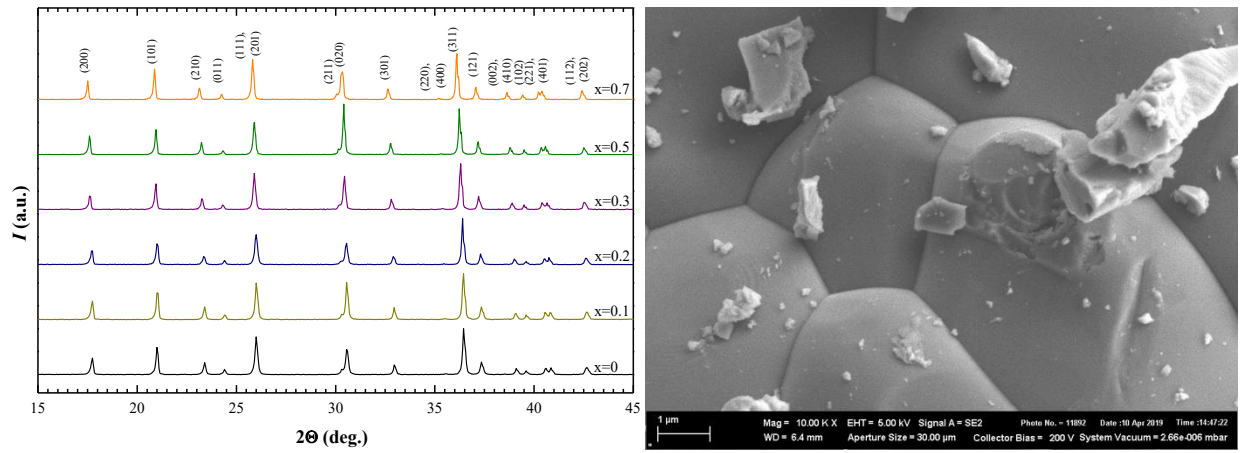


Figure 1. XRD-patterns for $\text{LiNi}_{1-x}\text{Co}_x\text{PO}_4$ (left). SEM-image of $\text{LiNi}_{0.6}\text{Co}_{0.4}\text{PO}_4$ (right).

above 0.5. This behavior of T_{C-IC} in the $\text{LiNi}_{1-x}\text{Co}_x\text{PO}_4$ is explained by the magnetic orderings competition, since in the compounds with $x = (0, 1)$ in which the spins are oriented along the c - and b -axis for LiNiPO_4 , and LiCoPO_4 , respectively.

Table 1. Unit cell parameters of crystal structure of the $\text{LiNi}_{1-x}\text{Co}_x\text{PO}_4$, and their temperature of magnetic phase transition from the commensurate to the incommensurate antiferromagnetic structures.

x	Sample	a (Å)	b (Å)	c (Å)	χ^2 (%)	T_{C-IC} (K)
0	LiNiPO_4	10.0335(6)	5.8581(3)	4.6785(3)	1.77	21.81(2)
0.1	$\text{LiNi}_{0.91}\text{Co}_{0.09}\text{PO}_4$	10.0513(6)	5.8646(3)	4.6811(3)	2.01	20.47(2)
0.2	$\text{LiNi}_{0.81}\text{Co}_{0.19}\text{PO}_4$	10.0697(6)	5.8722(4)	4.6839(3)	1.59	19.10(3)
0.3	$\text{LiNi}_{0.71}\text{Co}_{0.29}\text{PO}_4$	10.0836(6)	5.8782(3)	4.6859(3)	1.61	17.58(3)
0.5	$\text{LiNi}_{0.52}\text{Co}_{0.48}\text{PO}_4$	10.1175(4)	5.8911(2)	4.6899(2)	2.41	14.50(3)
0.7	$\text{LiNi}_{0.32}\text{Co}_{0.68}\text{PO}_4$	10.1504(5)	5.9024(2)	4.6937(2)	1.96	18.13(3)

This work was supported by MES of RF (contract No. 3.6121.2017/8.9), Act 211 Government of RF (contract No. 02.A03.21.0006), and supported in part by FASO of Russia (theme “Flux” No. AAA-A18-118020190112-8). The equipment of the Ural Center for Shared Use “Modern nanotechnology” SNSM UrFU was used.

1. J.-P. Rivera, *Ferroelec.* **161**, 147 (1994).
2. D. Vaknin, J.L. Zarestky, et. al, *Phys. Rev. Lett.* **92**(20), 207201 (2004).
3. I. Kornev, M. Bichurin, et. al, *Phys. Rev. B.* **62**(18), 12247 (2000).
4. R. Toft-Petersen, J. Jensen, et. al, *Phys. Rev. B.* **84**, 054408 (2011).
5. D. Vaknin, J.L. Zarestky, et. al, *Phys. Rev. B.* **60**(2), 1100 (1999).
6. R. Toft-Petersen, N.H. Andersen, et. al, *Phys. Rev. B.* **85**, 224415 (2012).
7. E. Fogh, R. Toft-Petersen, et. al, *Phys. Rev. B* **96**, 104420 (2017).